

The Antiferromagnetic Band Structure of La_2CuO_4 Revisited

Jason K. Perry,^{1,2} Jamil Tahir-Kheli,^{1,2} and William A. Goddard III²

¹*First Principles Research, Inc.*

8391 Beverly Blvd., Suite #171, Los Angeles, CA 90048

²*Materials and Molecular Simulation Center, Beckman Institute*

California Institute of Technology, Pasadena, CA 91125

Abstract. Using the Becke-3-LYP functional, we have performed band structure calculations on the high temperature superconductor parent compound, La_2CuO_4 . For the restricted spin paramagnetic case ($\rho_\uparrow = \rho_\downarrow$), the B3LYP band structure agrees well with the standard LDA band structure. It has a metallic ground state with a single $\text{Cu } x^2 - y^2 / \text{O } p_\sigma$ band crossing the Fermi level. For the unrestricted spin case ($\rho_\uparrow \neq \rho_\downarrow$), a spin polarized antiferromagnetic state is found with a band gap of 2.0 eV, agreeing well with experiment. This state is 1.0 eV (per formula unit) *lower* than the calculated paramagnetic state. This large energy difference is particularly startling given that the ferromagnetic state is also calculated to be 0.82 eV lower than the paramagnetic state. The apparent high energy of the spin restricted state is attributed to an overestimate of on-site Coulomb repulsion which is corrected in the unrestricted spin calculations. The stabilization of the total energy with spin polarization arises primarily from the stabilization of the $x^2 - y^2$ band, such that the character of the eigenstates at the top of the valence band in the antiferromagnetic state becomes a strong mixture of $\text{Cu } x^2 - y^2 / \text{O } p_\sigma$ and $\text{Cu } z^2 / \text{O}' p_z$. Since the Hohenberg-Kohn theorem requires the spin restricted and spin unrestricted calculations give exactly the same ground state energy and total density, this large disparity in energy reflects the inadequacy of current functionals for describing the cuprates. It seriously calls into question the use of any present-day restricted spin density functional band structure (including LDA) as a basis for single band theories of superconductivity in these materials.

INTRODUCTION

Almost immediately following the discovery of the superconducting cuprates (*e.g.* $\text{La}_{1-x}\text{Ba}_x\text{CuO}_4$ in 1986), several research groups characterized their band structures within the density functional (DFT) formalism.^{1–3} Using the standard local density approximation (LDA), the resulting paramagnetic (PM) band structures consistently showed the Fermi level behavior of these materials to be characterized by a single metallic 2-D band, comprised of $\text{Cu } x^2 - y^2 / \text{O } p_\sigma$ hybrid orbitals (from here on called the $x^2 - y^2$ band). All other occupied bands were buried 1 eV or more below the Fermi level. While the basic orbital picture appeared to agree with some experimental data, the absence of antiferromagnetic (AF) order in the band structure was cause for concern. In time, the inability of this band structure to explain an increasingly diverse range of normal state phenomena led many to conclude that Fermi liquid theory is not applicable to these materials. Indeed, no major theories based solely on this conventional band structure have survived. Still, the LDA band structure is widely viewed as a reasonable starting point for superconductivity theories and experimental data is routinely compared to these calculations.

In the early 1990's, a number of groups succeeded in computing an alternative AF state for undoped La_2CuO_4 within the DFT formalism. Using a pseudopotential approach, Shiraishi, *et al.*⁴ achieved a spin polarized solution where \uparrow and \downarrow spins reside on different Cu sites of a doubled unit cell. This opened up a band gap of 0.6 eV between occupied and unoccupied bands (the measured gap is 2.0 eV⁵). Other groups attempted to correct certain known flaws in the LDA functional. Most notably, Svane⁶ applied a self-interaction correction local spin density (SIC-LSD) approach, in which the residual Coulomb interaction an electron improperly sees with itself is removed from the LSD functional. Spin localization was achieved with this method and an AF band structure was found with an indirect band gap of 1.04 eV. Temmerman, *et al.*⁷ later found similar results using an alternative SIC-LSD approach. They reported an improved band gap of 2.1 eV. Czyzyk and Sawatzky⁸ took yet another approach (LSDA+U), embedding a Hubbard Hamiltonian into the Kohn-Sham LDA equation. They also achieved an AF state with a band gap of

1.65 eV.

A common characteristic of all these calculations was a significant change in orbital character near the top of the valence band as compared to the standard LDA band structure. All of the above authors noted a large increase in either the apical oxygen (O') or $Cu z^2$ density of states. While these results suggested the single band ($x^2 - y^2$) picture of LDA may not be an adequate starting point for the doping range of superconductivity, it was not immediately apparent that a more complicated band picture was consistent with the experimental data either. Unresolved was the difficult question of how to describe the doped state of the superconductor which appears to produce a Fermi surface in the Brillouin zone of the single unit cell.⁹ Removing electrons from a rigid band structure may be appropriate with the standard metallic state, but this procedure is less clear when starting from the undoped spin polarized insulating band structure in the reduced Brillouin zone (doubled unit cell). Thus, the LDA band structure has remained the de facto standard in the field to this day.

In this work, we revisit the DFT band structure using the Becke-3-Lee-Yang-Parr (B3LYP) functional.¹⁰ The superiority of this functional in describing molecular systems is well documented, but it is still relatively little used in band structure theory because it requires computation of the exact Hartree-Fock exchange. We find an AF B3LYP band structure in agreement with the results cited above, assuaging doubts about that work and confirming once again the significance of $Cu z^2/O' p_z$ character at the Fermi level. Most importantly, the AF state is found to be 1.0 eV per formula unit more stable than the PM state. Considering the Hohenberg-Kohn theorem¹¹ requires the exact spin restricted and spin unrestricted total densities and total energies to be equal, this discrepancy reveals a serious flaw in current functionals (B3LYP and LDA). Use of the LDA band structure to justify single band models of superconductivity in the cuprates is therefore highly questionable.

RESULTS AND DISCUSSION

Calculations were performed using CRYSTAL98¹² which employs an atomic Gaussian

type orbital basis set. For O, the standard 8-411G basis set with a D polarization exponent of 0.65 was used.¹³ For Cu and La, the Hay and Wadt¹⁴ effective core potentials (ECP's) were used. These ECP's treat explicitly the outer core (3s and 3p for Cu, 5s and 5p for La) and valence electrons. The basis sets used with these ECP's were modified from the original basis sets of Hay and Wadt, since some functions are too diffuse for calculations on crystals. For Cu, the two diffuse S exponents were replaced by a single exponent optimized to 0.30 from LDA calculations on La_2CuO_4 . The two Cu diffuse P exponents were replaced by a single exponent optimized to 0.20. The basis set was contracted to (3s3p3d) based on atomic Cu(II) calculations. For La, the two diffuse S exponents were replaced with a single exponent optimized to 0.10. The two diffuse P exponents and the diffuse D exponent were removed without replacement. The basis set was contracted to (3s2p1d) based on atomic La(III) and La(II) calculations. Overall, the quality of the basis set is superior to that used by Su, *et al.*¹⁵ in their CRYSTAL95 Hartree-Fock (HF) study of La_2CuO_4 . Several alternative basis sets were tested, all leading to similar results. The tetragonal La_2CuO_4 crystal structure was taken from Hazen.¹⁶

There are three primary states to consider in these calculations. The first is the antiferromagnetic (AF) state in which \uparrow and \downarrow spins localize to different Cu centers of the orthorhombic doubled unit cell. This is the ground state of undoped La_2CuO_4 . The second state is the ferromagnetic (FM) state, where \uparrow spins localize to all Cu centers under tetragonal symmetry. The last is the paramagnetic (PM) state, where spin is disordered and each Cu site could be either \uparrow or \downarrow spin. A transition to this latter state is expected upon doping.

In Figure 1, we present the results of our LDA and B3LYP calculations with restricted spin and tetragonal symmetry. The results meet our basic expectations of the PM state. The LDA band structure is in excellent agreement with previous plane wave calculations¹⁻³ and there is little difference with the B3LYP band structure result. Both methods find the only band crossing the Fermi level is the highly 2-D $x^2 - y^2$ band. The next band (z^2) is more than 1 eV below the Fermi level.

An analysis of the density of states (Figure 2) shows the nature of the intrinsic

undoped hole (lowest unoccupied states totaling 1 electron) is 48% $Cu x^2 - y^2$ and 47% $O p_\sigma$. While we have not carried out computations on the doped state ($x=0.15$), using a rigid band model we can estimate the nature of the doped hole. The character of this doped hole (highest occupied states totaling 0.15 electron) is 47% $Cu x^2 - y^2$, 38% $O p_\sigma$, 6% $O' p_z$, and 5% $Cu z^2$. The relatively small amount of O' and z^2 character in these orbitals is in keeping with most models for superconductivity in the cuprates. However, x-ray absorption studies (XAS) support a total z^2 hole contribution of anywhere from 5%-20% and a similar range for $O' p_z$.¹⁷ Furthermore, while the calculated Fermi surface appears to be in good agreement with the ARPES, the band dispersion is a bit too broad.⁹

Details such as the ARPES pseudogap,¹⁸ the anomalous background signal,¹⁹ and other probes of the normal state properties such as the NMR,²⁰ resistivity,²¹ and neutron scattering²² also appear to have no explanation using this conventional band structure. Finally, the lack of antiferromagnetic order is clearly a major shortcoming.

In Figure 3, we present results of unrestricted spin (UB3LYP) calculations using an orthorhombic unit cell. The combination of a spin functional and a doubled unit cell allows for a possible spin polarized solution. Indeed, an AF state with a gap of 2.0 eV is found. The band dispersion is in excellent agreement with previously published DFT band structures for this AF state,⁶⁻⁸ and the computed gap agrees with the measured gap.⁵ Unlike previous attempts though, this band structure was arrived at unambiguously using a well established functional. No empirical corrections were necessary. While no comparison of the relative stabilities of the LDA PM state and the SIC-LSD (or LSDA+U) AF state has been previously reported, with these calculations a comparison is rather straightforward. Perhaps surprisingly, we find the UB3LYP AF state is 1.0 eV per formula unit more stable than the B3LYP PM state.

This added stability of the AF state is associated with a stabilization of the $x^2 - y^2$ band with respect to the other bands. In Figure 4, we show the density of states for the AF state. From this we characterize the nature of the undoped hole as 56% $Cu x^2 - y^2$ and 38% $O p_\sigma$. This picture is not substantially different from that obtained with the PM

B3LYP calculation. The ratio of $Cu\ x^2 - y^2/O\ p_\sigma$ character is somewhat larger in the AF state, but qualitatively both calculations agree the undoped hole states are nearly purely derived from these two orbitals. The picture changes dramatically upon considering the nature of the doped holes. Figure 5 presents a detail of the density of states in the vicinity of the Fermi level for the $x=0.15$ doped state, assuming a rigid band model. The nature of the doped hole can be characterized as 17% $Cu\ x^2 - y^2$, 40% $O\ p_\sigma$, 21% $O'p_z$, and 19% $Cu\ z^2$. This is summarized in Table I. The significant increase in the $Cu\ z^2$ and $O' p_z$ character of the doped hole as compared to the B3LYP PM results is comparable to that noted in previous AF band structure calculations.^{4,6-8} While doubts about the quality of the previous band structures undermined the significance of these findings, the cumulative weight of these results now strongly favors the scenario where z^2 holes are formed upon doping.

To understand why the PM and AF band structures differ so strongly in this regard, one must understand that the restricted spin B3LYP, and by extension, the LDA, have failed to produce the proper ground state. The Hohenberg-Kohn theorem¹⁰ proves the existence of two functionals $F_{HK}[\rho]$ and $F_{HK}[\rho_\uparrow, \rho_\downarrow]$ where the first is a functional of the total density $\rho = \rho_\uparrow + \rho_\downarrow$ and the second is a functional of the two spin densities ρ_\uparrow and ρ_\downarrow . The Kohn-Sham orbitals arising from energy minimization for La_2CuO_4 will be of restricted (doubly occupied) Hartree-Fock type for $F_{HK}[\rho]$ with $\rho(r) = 2 \sum_{occ} |\phi_i(r)|^2$ and unrestricted Hartree-Fock type for $F_{HK}[\rho_\uparrow, \rho_\downarrow]$ where the \uparrow spin orbitals may be different from the \downarrow spin orbitals. Both minimizations should lead to exactly the same energy and ground state total density ρ . Thus, if the B3LYP functional were close to $F_{HK}[\rho]$ and the UB3LYP functional were close to $F_{HK}[\rho_\uparrow, \rho_\downarrow]$, then the energy of the two calculations for La_2CuO_4 should be close to each other. It is well known that spin density functional approximations to $F_{HK}[\rho_\uparrow, \rho_\downarrow]$ are superior to total density approximations to $F_{HK}[\rho]$ since it is much easier to empirically design functionals to correct for the exchange coupling of like spins when ρ is separated into ρ_\uparrow and ρ_\downarrow .

A good test of whether spin restricted B3LYP is a good functional is to compare the

energy of the FM state, which has a pure \uparrow spin per formula unit, to the PM and AF states. For La_2CuO_4 , one would expect the energy of the AF and FM states to differ on the order of 0.13 eV (the order of the experimental AF coupling J).²³ We find the energy difference to be 0.18 eV with the UB3LYP functional. This good agreement is in marked contrast to the results for the PM state. The B3LYP PM state should be expected to be between the AF and FM states (indeed, strictly equivalent to the AF state), but we find instead the PM state is 0.82 eV per formula unit higher than the FM state and 1.0 eV higher than the AF state. This is clearly nonsense. The implications of this are not just that the restricted spin calculation hasn't found the correct AF ground state, it hasn't even found the correct PM state.

As many have argued elsewhere, a major problem with DFT calculations on the PM state is that they don't properly describe the correlations between spins on neighboring sites. While that is clearly a concern, a larger problem is that when the \uparrow and \downarrow spin densities are constrained to be the same, as they are in the PM state, the on-site Coulomb repulsion between spins is overestimated within the half-occupied metallic band. These calculations do not represent a spin-disordered state where each site can have a spin of either \uparrow or \downarrow ; they represent a spin-averaged state where each site is non-magnetic. This leads to an on-site repulsion between \uparrow spins and \downarrow spins which is inappropriate in these strongly correlated systems.

A classic example of the problems that occur with these functionals is the dissociation of H_2 . At equilibrium distances, the molecule is well described by closed-shell LDA or B3LYP functionals. However, at the dissociation limit the ionic component ($\text{H}^+ + \text{H}^-$) is not entirely eliminated and the energy is calculated to be too high with respect to two H atoms. Only calculation of either the triplet state or the symmetry broken unrestricted spin state allows the formation of magnetic moments on each H atom and a proper description of dissociation. *This difference should not be considered a failure of molecular orbital theory or even density functional theory. Instead, it is a failure of the empirical functionals that have been developed so far.*

By analogy, the FM state of undoped La_2CuO_4 (where each site has a pure \uparrow spin)

is well described as is the the AF state (where each site has either a pure \uparrow or a pure \downarrow spin). For the spin disordered PM state (each site is 50% \uparrow AND 50% \downarrow), this is not the case. The error is manifested not just in the total energy. The band dispersion is affected as well. In particular, the $x^2 - y^2$ band is elevated relative to the other bands as a result of the improper on-site Coulomb repulsion associated with the $Cu\ x^2 - y^2/O\ p_\sigma$ orbital. Removing this repulsion through the localization of spins in either the FM or AF states stabilizes the band, such that an increase in z^2 character near the top of the valence band is then observed.

While it may be tempting to conclude that Fermi liquid theory has failed for these materials, a simpler answer might just be that LDA has failed. The calculations presented here demonstrate the shortcomings of these methods and suggest possible solutions. Elsewhere, we have already incorporated the spin correlation described in this paper into a simple tight binding model for the PM state.²⁴ By effectively introducing a local magnetic moment at each Cu site within a spin-disordered model of optimally doped $La_{1.85}Sr_{0.15}CuO_4$, we have shown the $x^2 - y^2$ band is significantly stabilized relative to the other bands. This brings the narrow z^2 band to the Fermi level. The unique band structure, which is approximately a 2-D band ($x^2 - y^2$) crossing a 1-D band (z^2) normal to it, represents a dramatic first-order correction to the standard band structure. Detailed descriptions of the ARPES pseudogap and anomalous background,²⁵ the NMR Cu and O relaxations and Knight shifts,²⁶ the Hall effect, and Josephson tunneling²⁷ have already been presented with this model.

CONCLUSIONS

In summary, we have presented the results of B3LYP and UB3LYP band structure calculations on the PM and AF states of La_2CuO_4 . The results are in good agreement with previous LDA calculations on the PM state and SIC-LSD calculations on the AF state (among others). The large discrepancy in energy between the two states (1.0 eV per formula unit) can be attributed to an improper overestimate of on-site Coulomb repulsion within the spin restricted calculations. The automatic correction of this error within the AF state leads to the stabiliation of the $x^2 - y^2$ band relative to the other occupied bands. As a

result, the z^2 band is then brought the top of the valence band and contributes significantly to the doped hole states. These results cast significant doubt on the continued use of LDA band structures as the starting point for theories of superconductivity in these materials.

We wish to acknowledge helpful discussions with Dr. Francesco Faglioni and Dr. Eugene Heifets.

REFERENCES

- ¹ J. Yu, A.J. Freeman, and J.H. Xu, Phys. Rev. Lett. **58**, 1035 (1987).
- ² L.F. Mattheiss, Phys. Rev. Lett. **58**, 1028 (1987).
- ³ W.E. Pickett, Rev. Mod. Phys. **61**, 433 (1989).
- ⁴ K. Shiraishi, A. Oshiyama, N. Shima, T. Nakayama, and H. Kamimura, Solid State Commun. **66**, 629 (1988).
- ⁵ J.M. Ginder, R.M. Roe, Y. Song, R. P. McCall, J.R. Gaines, E. Ehrenfreund, and A.J. Epstein, Phys. Rev. B **37**, 7506 (1988).
- ⁶ A. Svane, Phys. Rev. Lett. **68**, 1900 (1992).
- ⁷ W.M. Temmerman, Z.Szotek, and H. Winter, Phys. Rev. B **47**, 11533 (1993).
- ⁸ M.T. Czyzyk and G.A. Sawatsky, Phys. Rev. B **49**, 14211 (1994).
- ⁹ A. Ino, C. Kim, T. Mizokawa, Z.-X. Shen, A. Fujimori, M. Takaba, K. Tamasaku, H. Eisaki, and S. Uchida, J. Phys. Soc. Japan **68**, 1496 (1999).
- ¹⁰ A.D. Becke, J. Chem. Phys. **98**, 5648 (1993); C. Lee, W. Yang, and R.G. Parr, Phys. Rev. B **37**, 785 (1988).
- ¹¹ P. Hohenberg and W. Kohn, Phys. Rev. **136**, B864 (1964).
- ¹² V.R. Saunders, R. Dovesi, C. Roetti, M. Causà, N.M. Harrison, R. Orlando, C.M. Zicovich-Wilson, *CRYSTAL98 User's Manual*, University of Torino, Torino, 1998.
- ¹³ <http://www.dl.ac.uk/TCS/Software/CRYSTAL>.
- ¹⁴ P.J. Hay and W.R. Wadt, J. Chem. Phys. **82**, 299 (1985).
- ¹⁵ Y.-S. Su, T.A. Kaplan, S.D. Mahanti, and J.F. Harrison, Phys. Rev. B **59**, 10521 (1999).

- ¹⁶ R.M. Hazen, in *Physical Properties of High Temperature Superconductors II*, ed. D.M. Ginsberg (World Scientific, New Jersey; 1990), 121-198.
- ¹⁷ N. Nücker, H. Romberg, X.X. Xi, J. Fink, B. Gegenheimer, and Z.-X. Shen, *Phys. Rev. B* **39**, 6619 (1989); A. Bianconi, S. Della Longa, C. Li, M. Pompa, A. Gongiu-Castellano, D. Udron, A. M. Flank, and P. Lagarde, *Phys. Rev. B* **44**, 10126 (1991); C.T. Chen, L.H. Tjeng, J. Kwo, H.L. Kao, P. Rudolf, F. Sette, and R.M. Fleming, *Phys. Rev. Lett.* **68**, 2543 (1992).
- ¹⁸ M.R. Norman, H. Ding, M. Randeria, J.C. Campuzano, T. Yokoya, T. Takeuchi, T. Takahashi, T. Mochiku, K. Kadowaki, P. Guptasarma, and D.G. Hinks, *Nature* **392**, 157 (1998).
- ¹⁹ Z.-X. Shen and D.S. Dessau, *Phys. Rep.* **253**, 2 (1995).
- ²⁰ R.E. Walstedt, B.S. Shastry, and S.-W. Cheong, *Phys. Rev. Lett.* **72**, 3610 (1994).
- ²¹ H. Takagi, B. Batlogg, H.L. Kao, J. Kwo, R.J. Cava, J.J. Krajewski, and W.F. Peck, Jr., *Phys. Rev. Lett.* **69**, 2975 (1992).
- ²² S.-W. Cheong, G. Aeppli, T.E. Mason, H. Mook, S.M. Hayden, P.C. Canfield, Z. Fisk, K.N. Clausen, and J.L. Martinez, *Phys. Rev. Lett.* **67**, 1791 (1991).
- ²³ G. Aeppli, S.M. Hayden, H.A. Mook, Z. Fisk, S.-W. Cheong, D. Rytz, J.P. Remeika, G.P. Espinosa, and A.S. Cooper, *Phys. Rev. Lett.* **62**, 2052 (1989); P.E. Sulewski, P.A. Fleury, K.B. Lyons, S.-W. Cheong, and Z. Fisk, *Phys. Rev. B* **41**, 225 (1990).
- ²⁴ J.K. Perry and J. Tahir-Kheli, *Phys. Rev. B* **58**, 12323 (1998); J.K. Perry, *J. Phys. Chem. A* **104**, 2438 (2000); J.K. Perry and J. Tahir-Kheli, unpublished (cond-mat/9907332).
- ²⁵ J.K. Perry and J. Tahir-Kheli, *Phys. Rev. B*, submitted (cond-mat/9908308).
- ²⁶ J. Tahir-Kheli, *J. Phys. Chem. A* **104**, 2432 (2000).
- ²⁷ J. Tahir-Kheli, *Phys. Rev. B* **58**, 12307 (1998).

Table I. Orbital character of intrinsic undoped holes (totaling 1 electron), doped holes (totaling 0.15 electron), and total holes at optimal doping (totaling 1.15 electron). Results are shown for both the restricted spin B3LYP paramagnetic state and unrestricted spin UB3LYP antiferromagnetic state.

Orbital	B3LYP			UB3LYP		
	undoped	doped	total	undoped	doped	total
<i>Cu</i> $x^2 - y^2$	48%	47%	48%	56%	17%	51%
<i>O</i> p_σ	47%	38%	46%	38%	40%	38%
<i>O'</i> p_z	1%	6%	2%	1%	21%	4%
<i>Cu</i> z^2	1%	5%	2%	0%	19%	3%

FIGURE CAPTIONS

Figure 1. Band dispersions plotted along symmetry lines of the tetragonal Brillouin zone (see reference 1) from restricted spin (a) LDA and (b) B3LYP calculations. Results are in good agreement with the LDA computations of references 1-3.

Figure 2. Density of states from the restricted spin B3LYP calculation. (a) projected Cu DOS vs. total DOS. (b) projected O DOS vs. total DOS. (c) projected O' DOS vs. total DOS. (d) projected Cu $x^2 - y^2$ DOS vs. total Cu DOS. (e) projected Cu z^2 DOS vs. total Cu DOS.

Figure 3. Band dispersion plotted along symmetry lines of the orthorhombic Brillouin zone (see reference 8) from the unrestricted spin UB3LYP calculation. Results are in good agreement with the SIC-LSD and LSDA+U computations of references 6-8.

Figure 4. Density of states from the unrestricted spin UB3LYP calculation. (a) projected Cu DOS vs. total DOS. (b) projected O DOS vs. total DOS. (c) projected O' DOS vs. total DOS. (d) projected Cu $x^2 - y^2$ DOS vs. total Cu DOS. (e) projected Cu z^2 DOS vs. total Cu DOS.

Figure 5. Detail of the density of states from the unrestricted spin UB3LYP calculation. Fermi level is positioned to a doping level of $x=0.15$. (a) projected Cu DOS vs. total DOS. (b) projected O DOS vs. total DOS. (c) projected O' DOS vs. total DOS. (d) projected Cu $x^2 - y^2$ DOS vs. total Cu DOS. (e) projected Cu z^2 DOS vs. total Cu DOS.

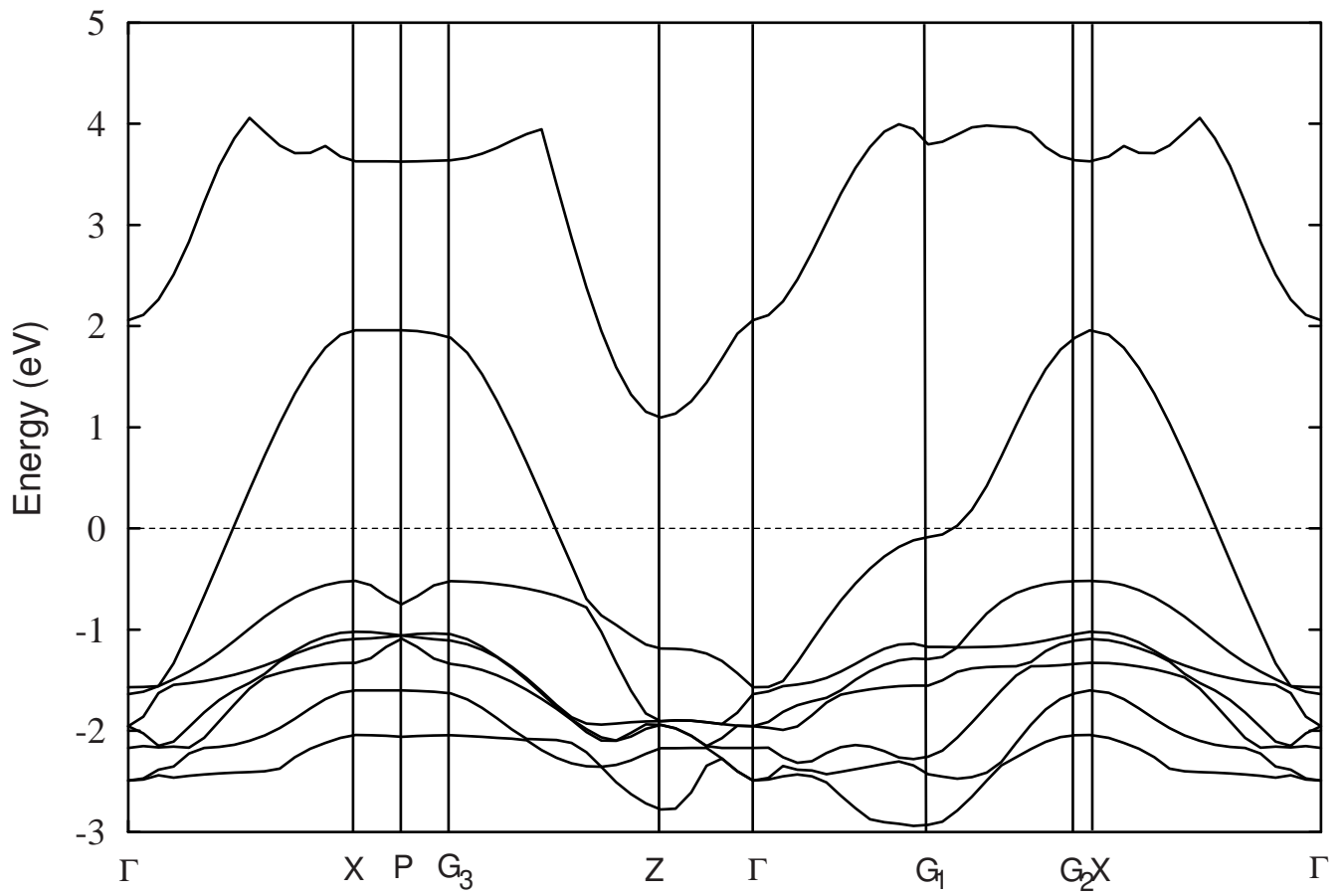


Figure 1a

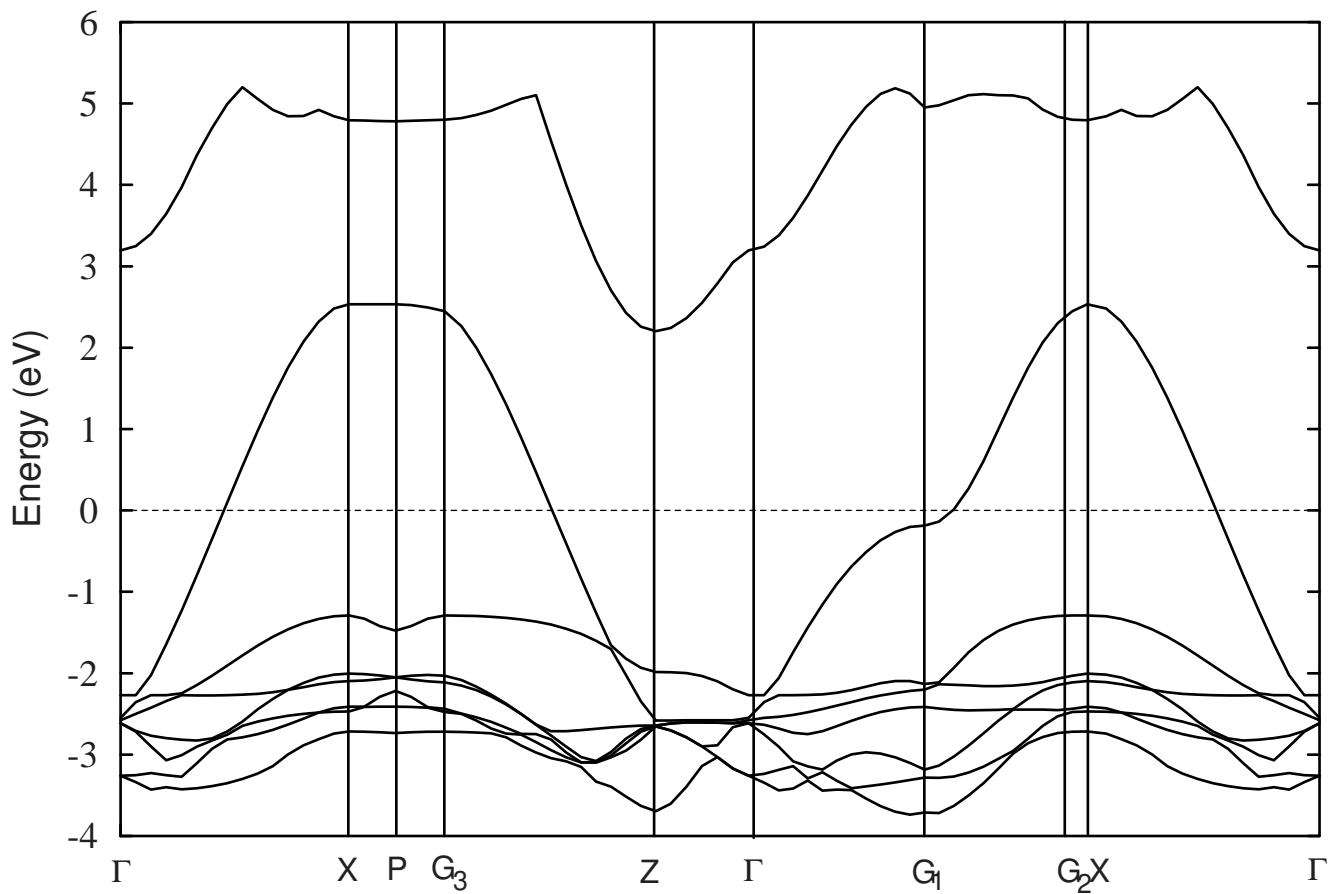


Figure 1b

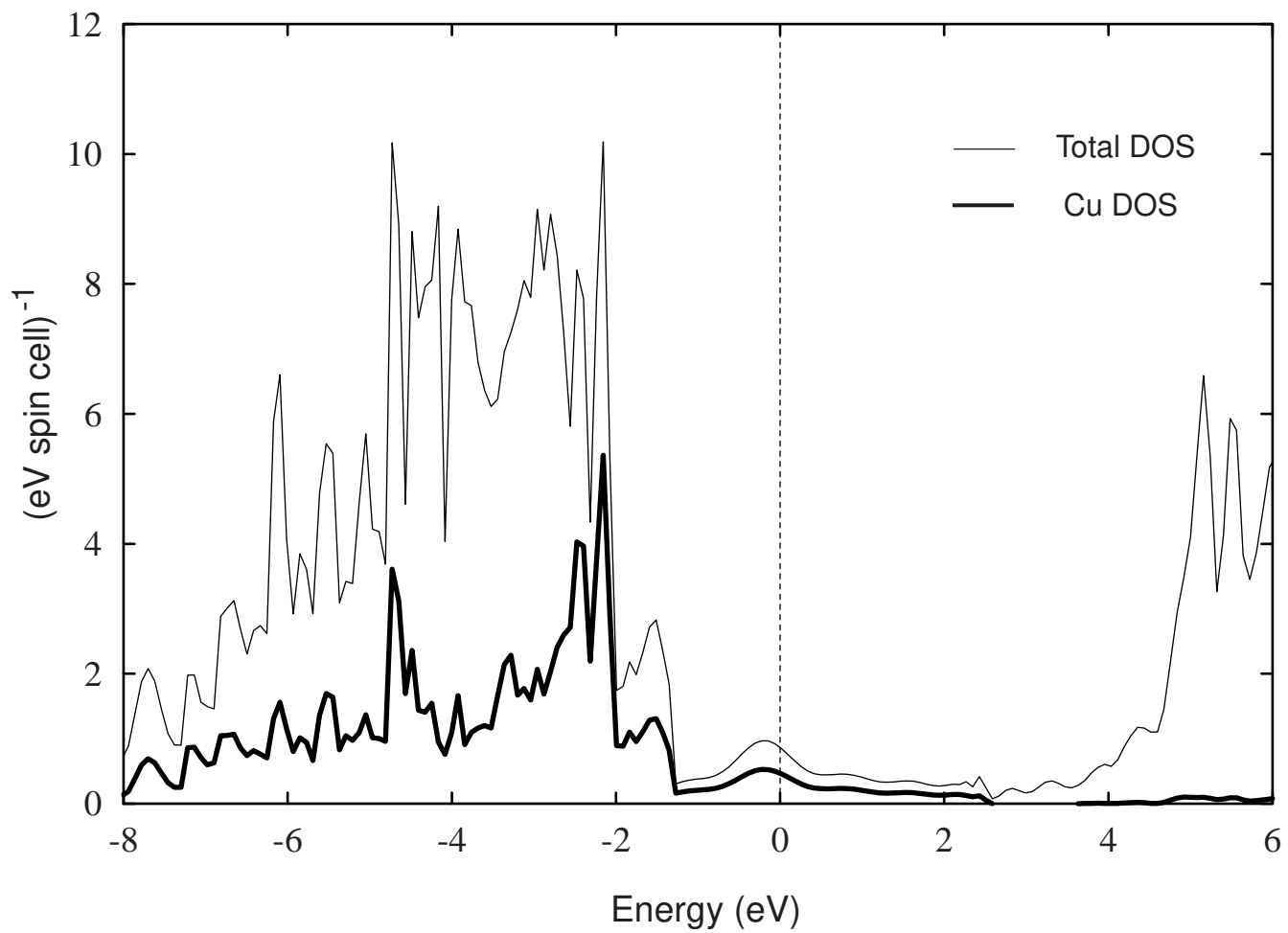


Figure 2a

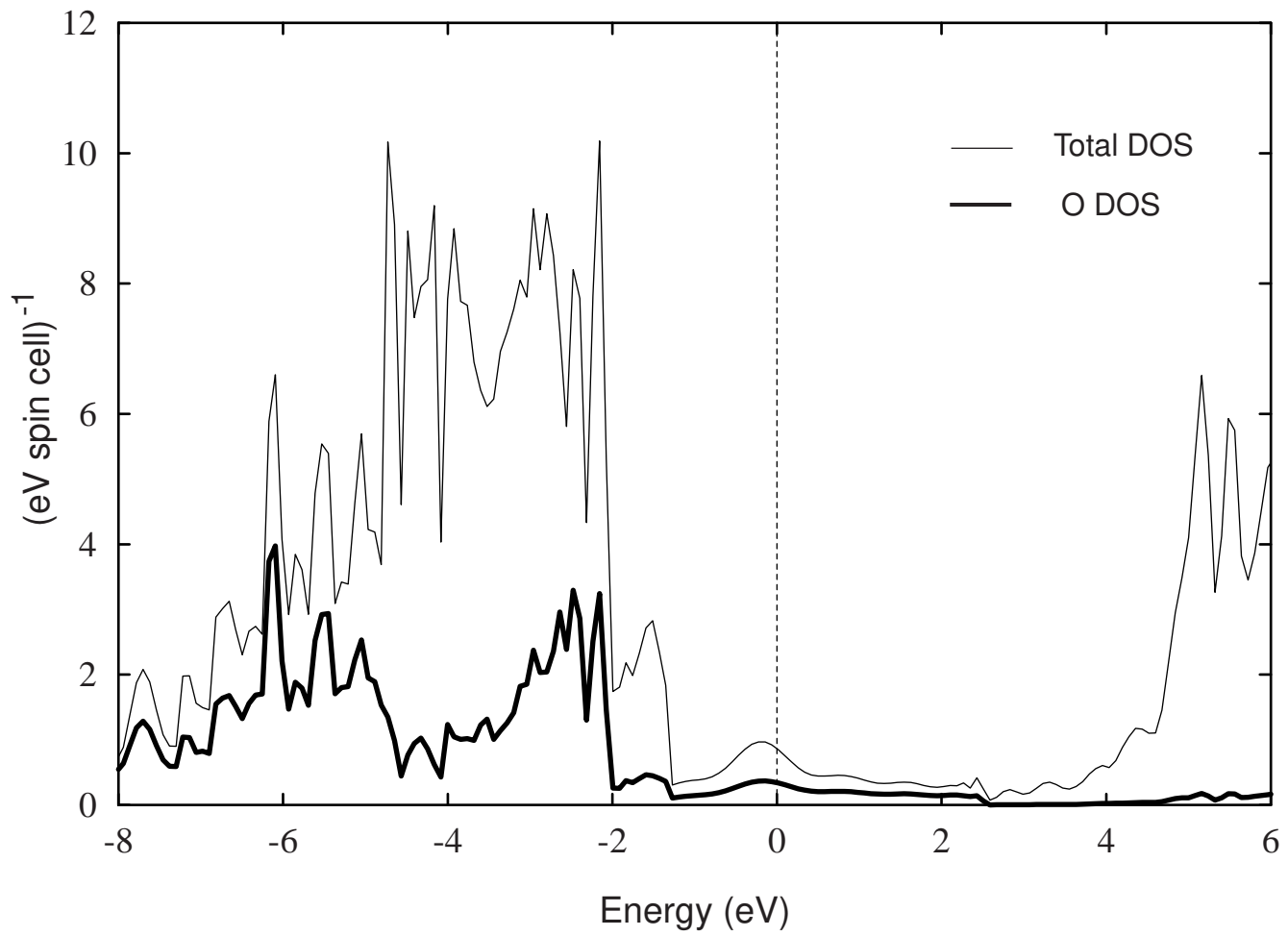


Figure 2b

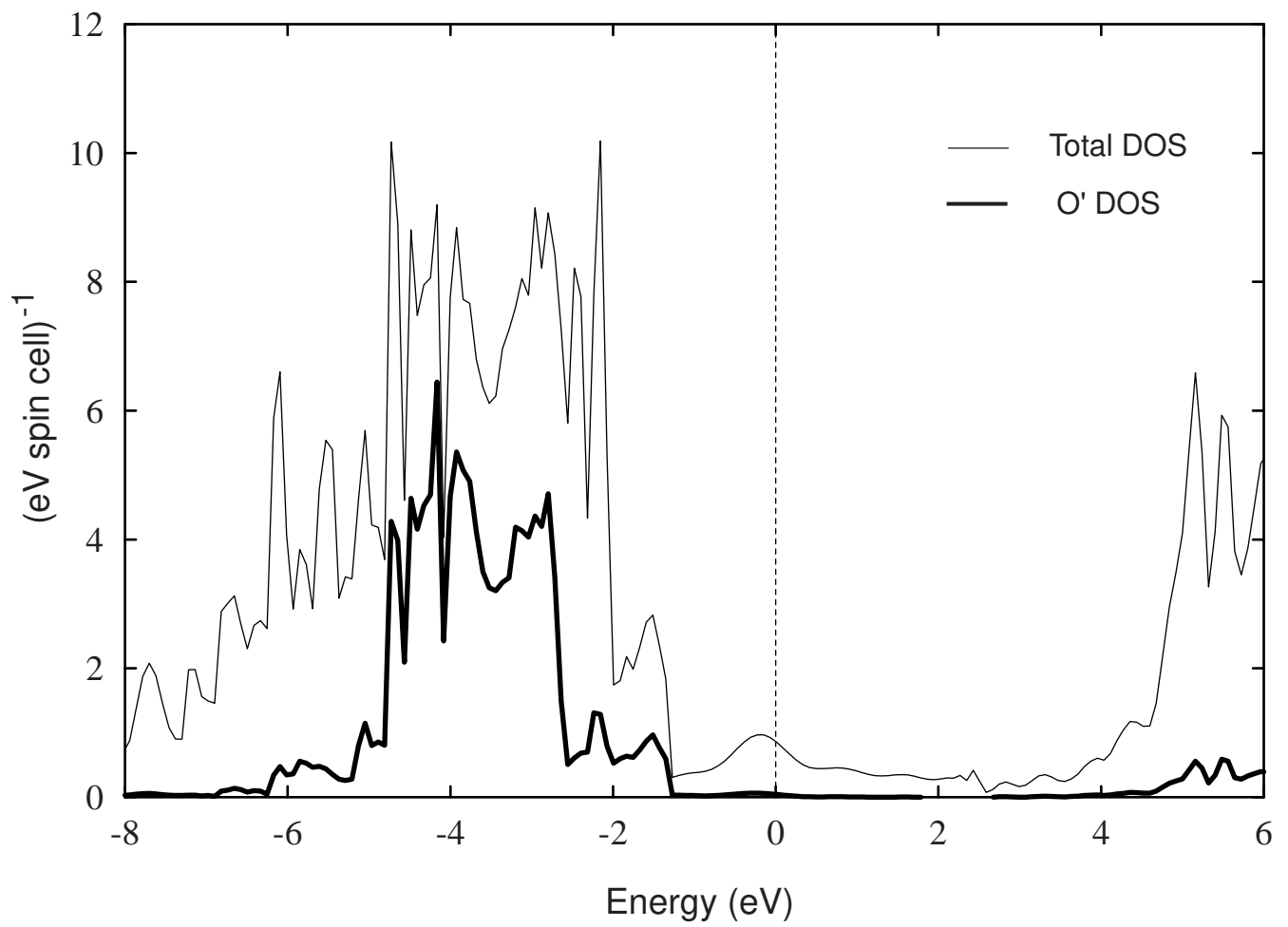


Figure 2c

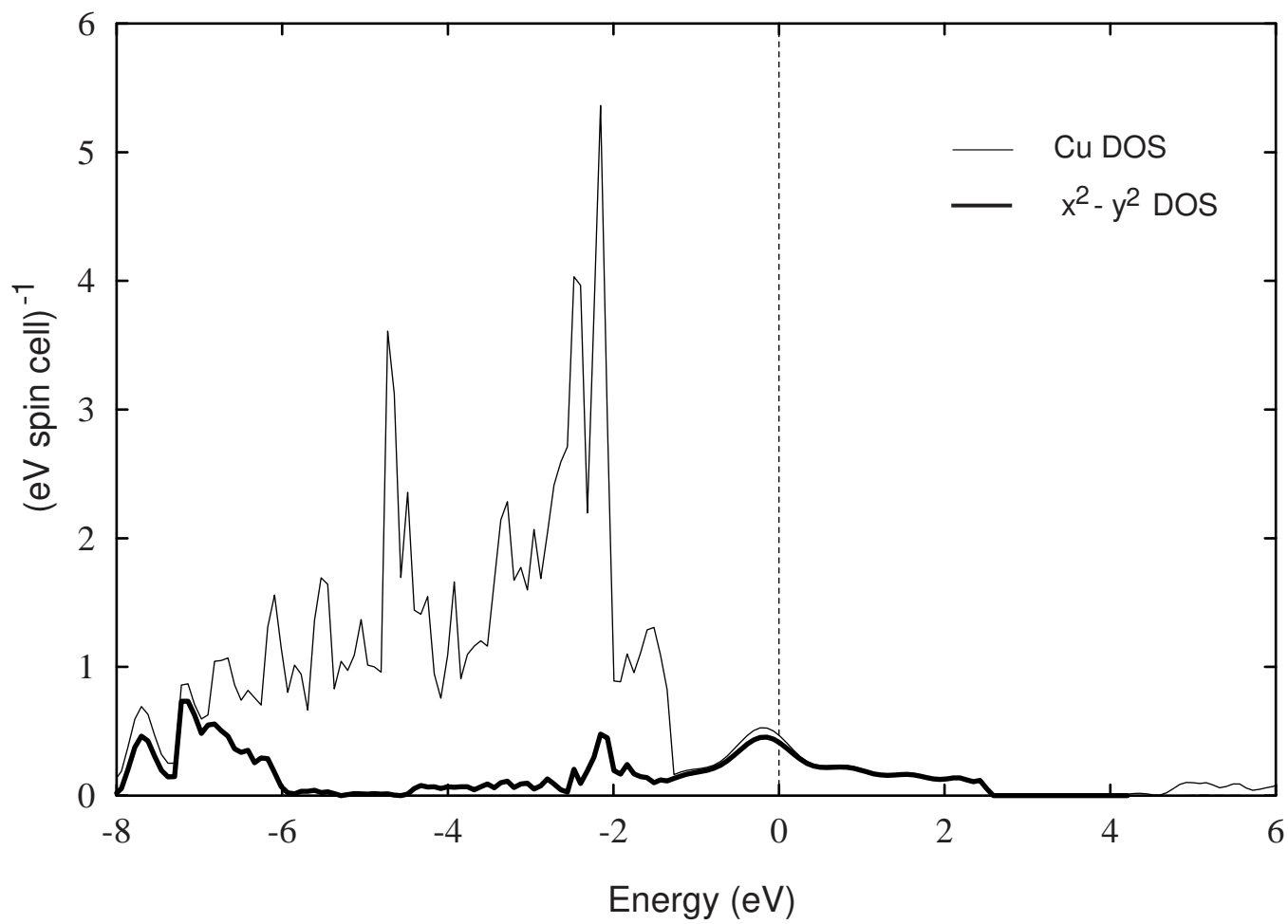


Figure 2d

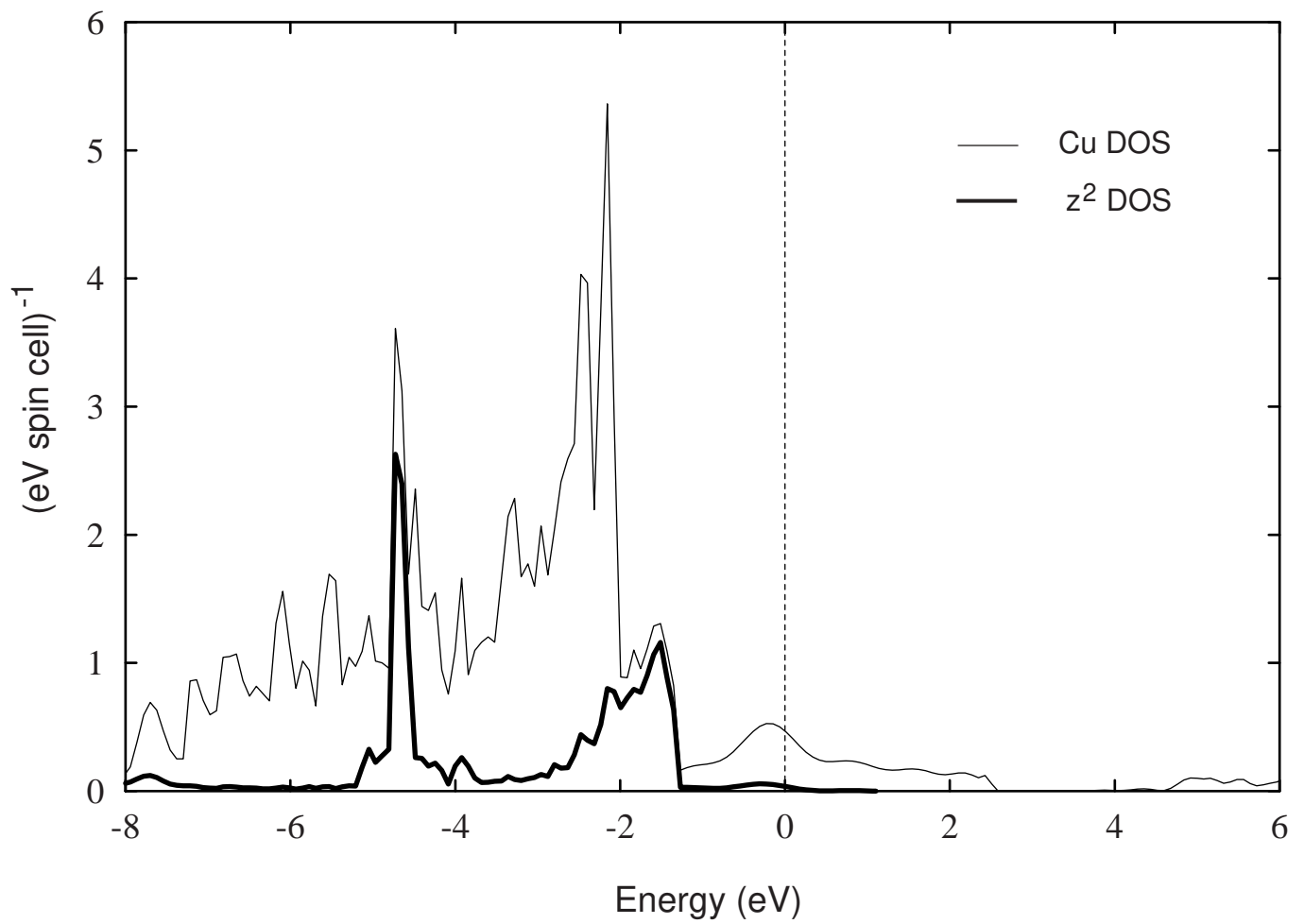


Figure 2e

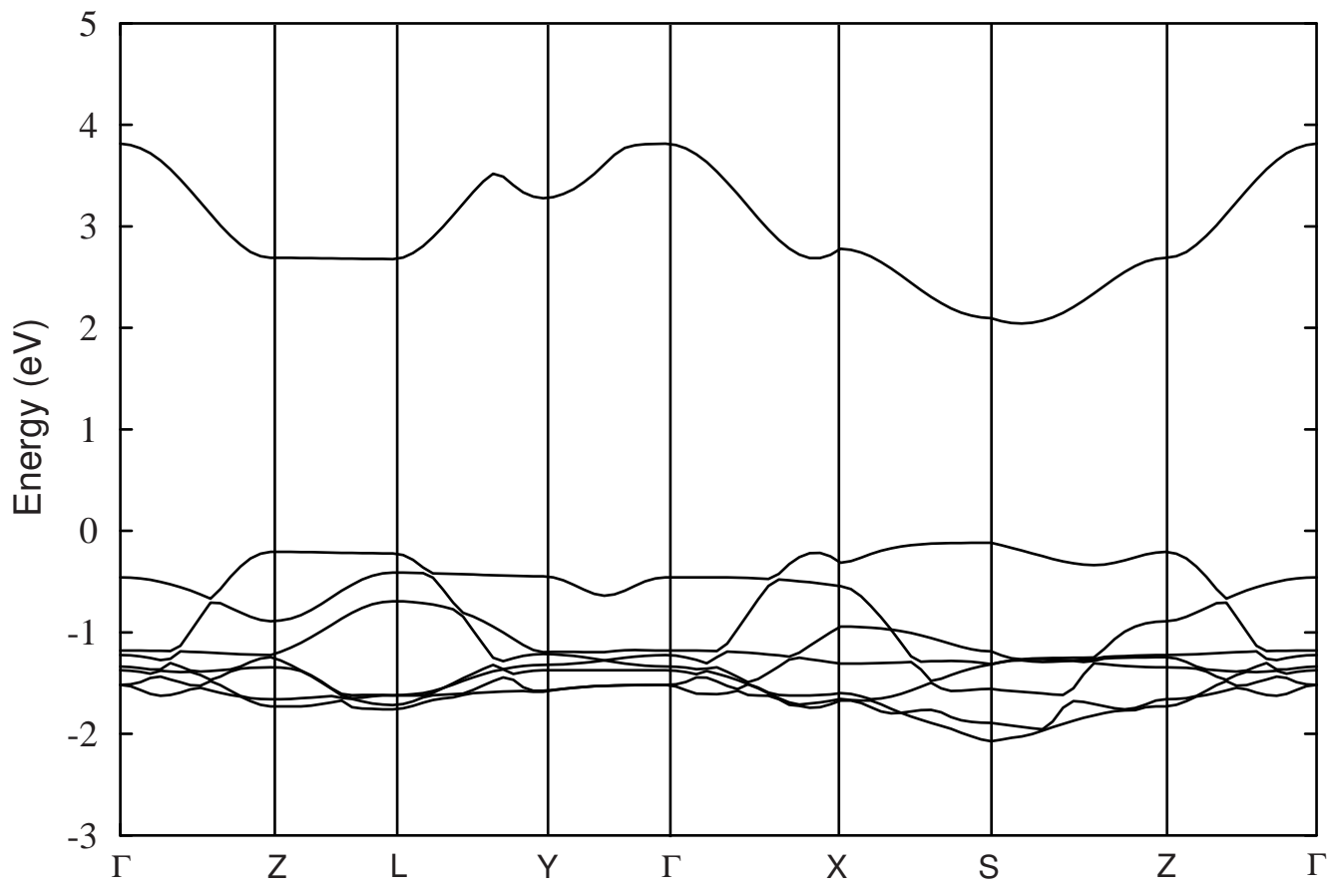


Figure 3

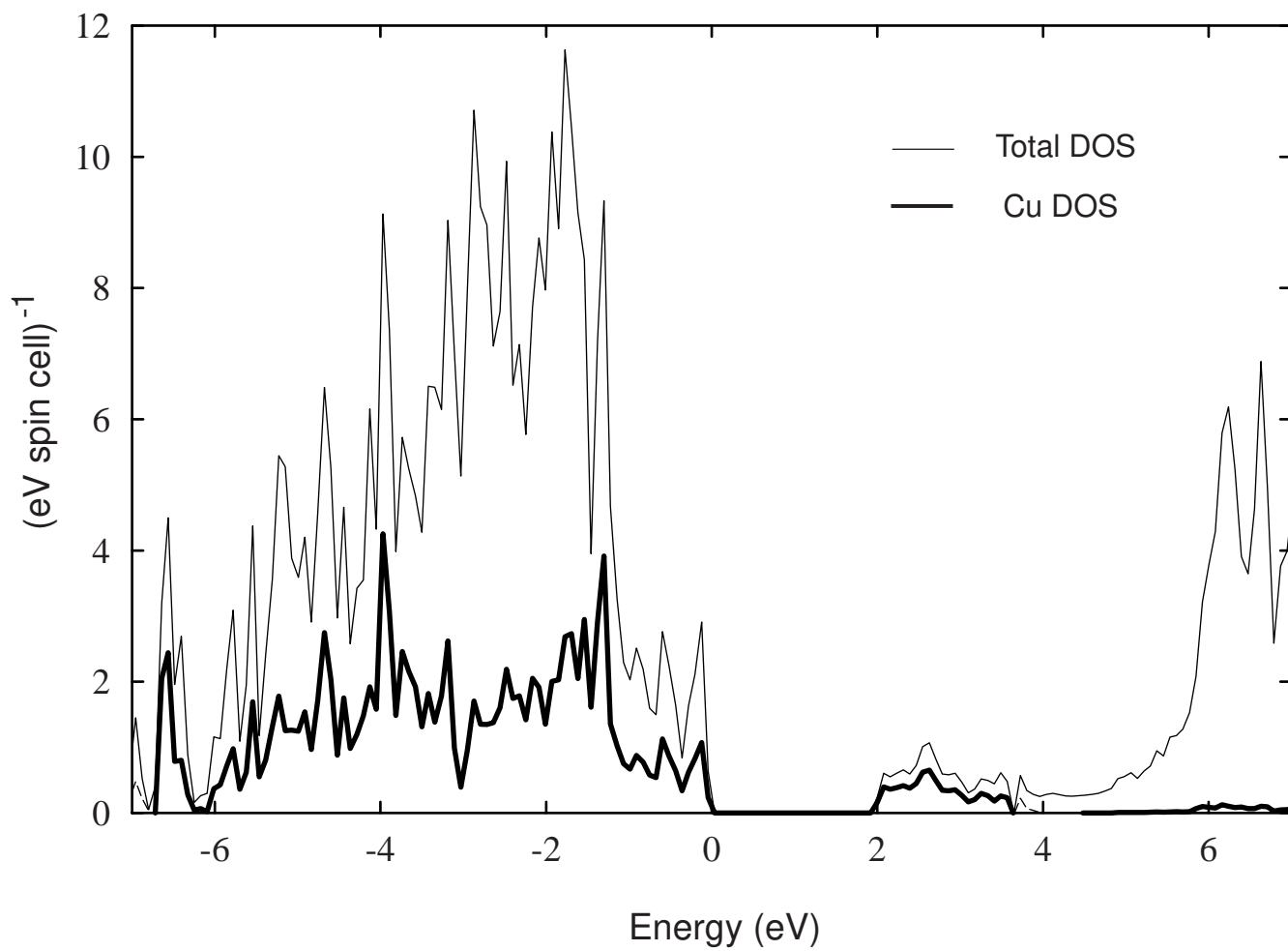


Figure 4a

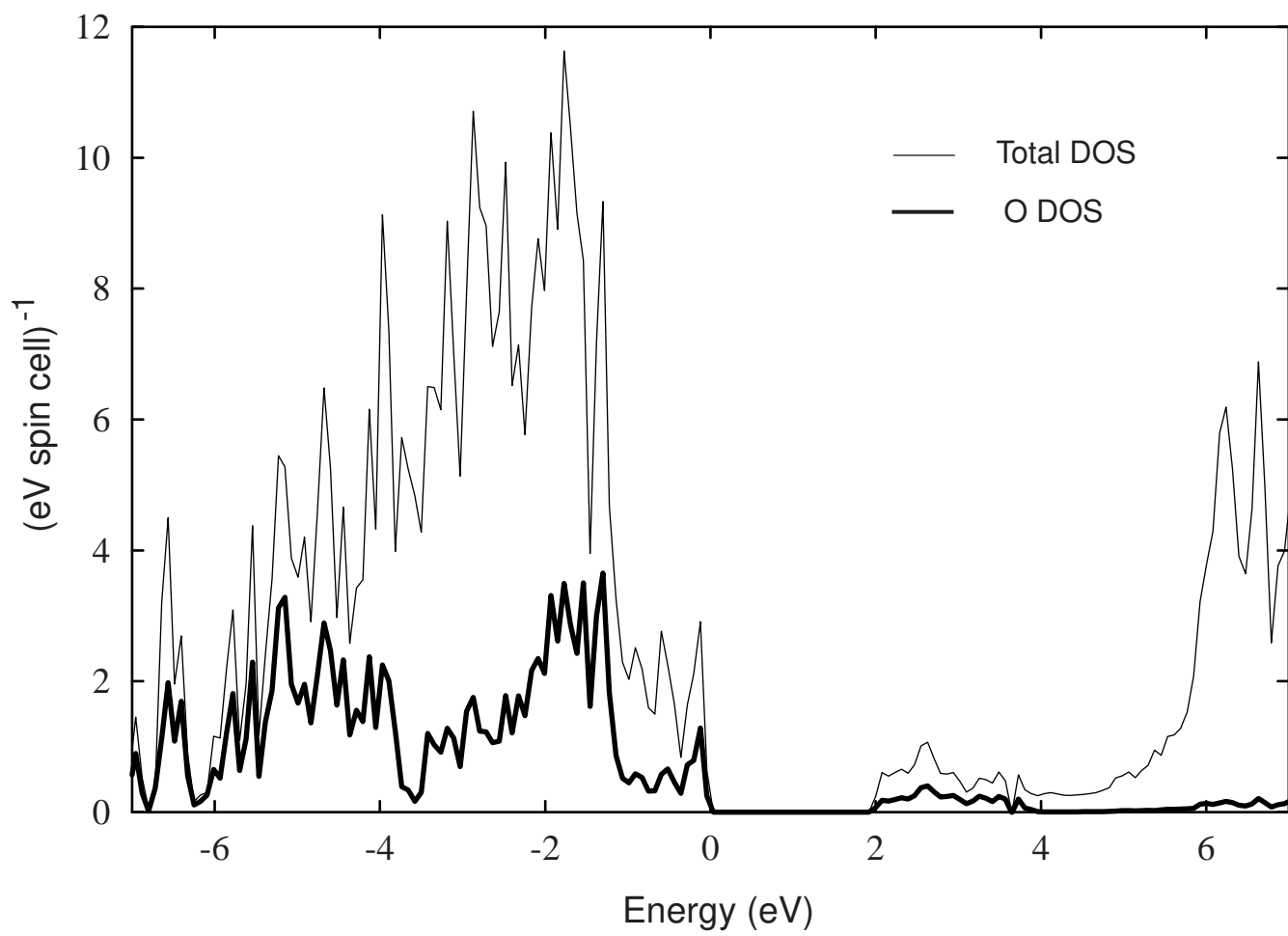


Figure 4b

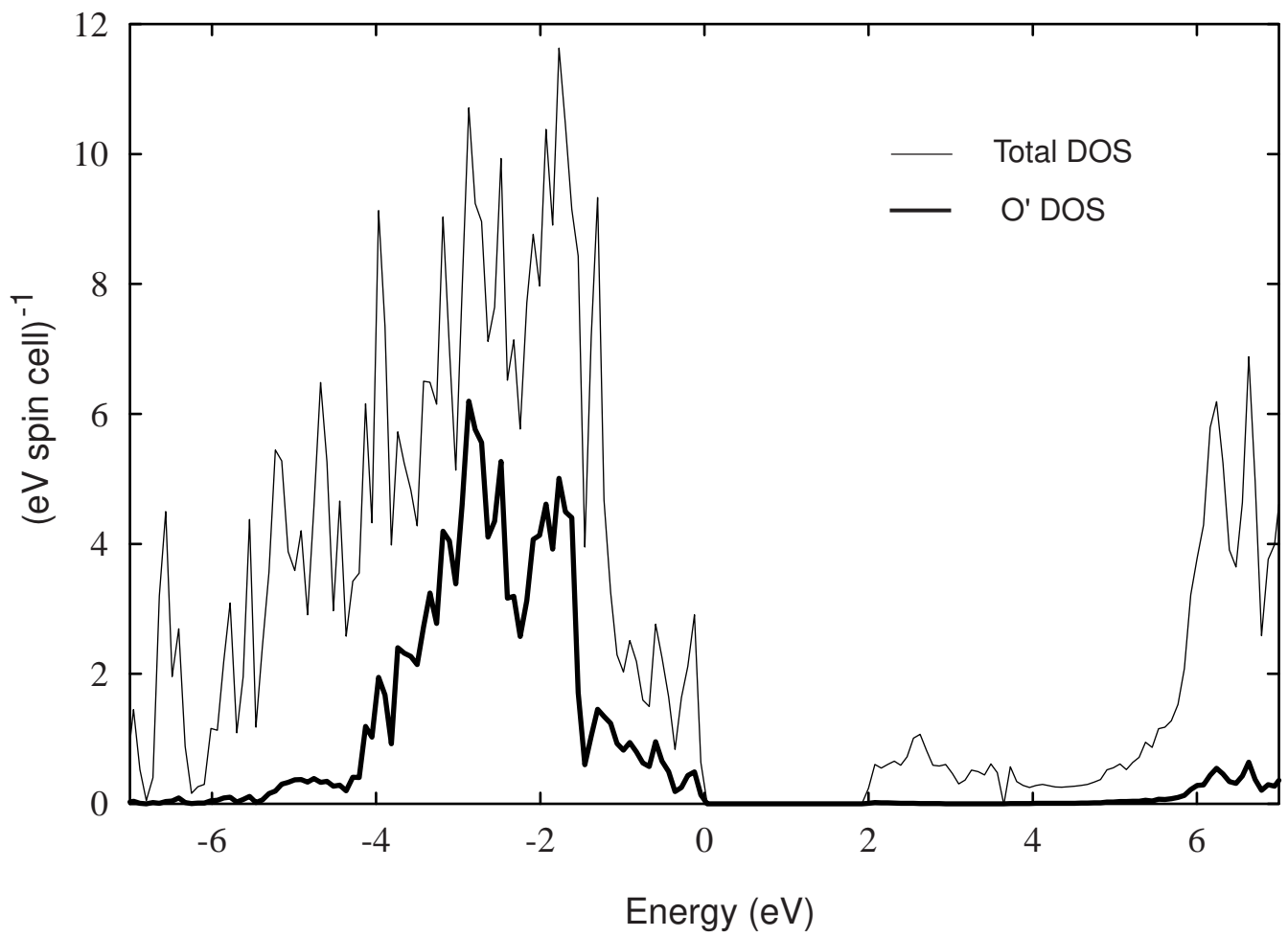


Figure 4c

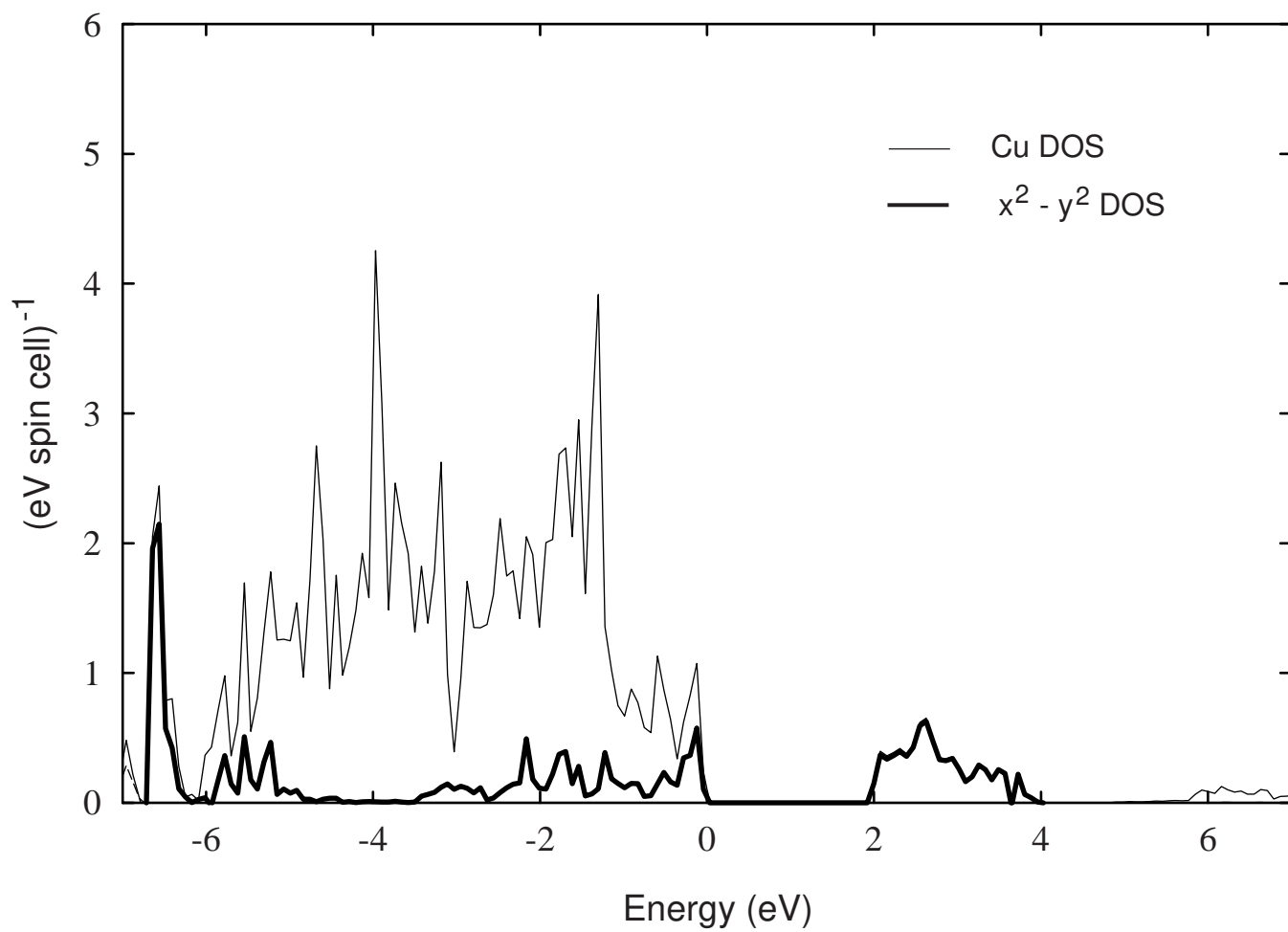


Figure 4d

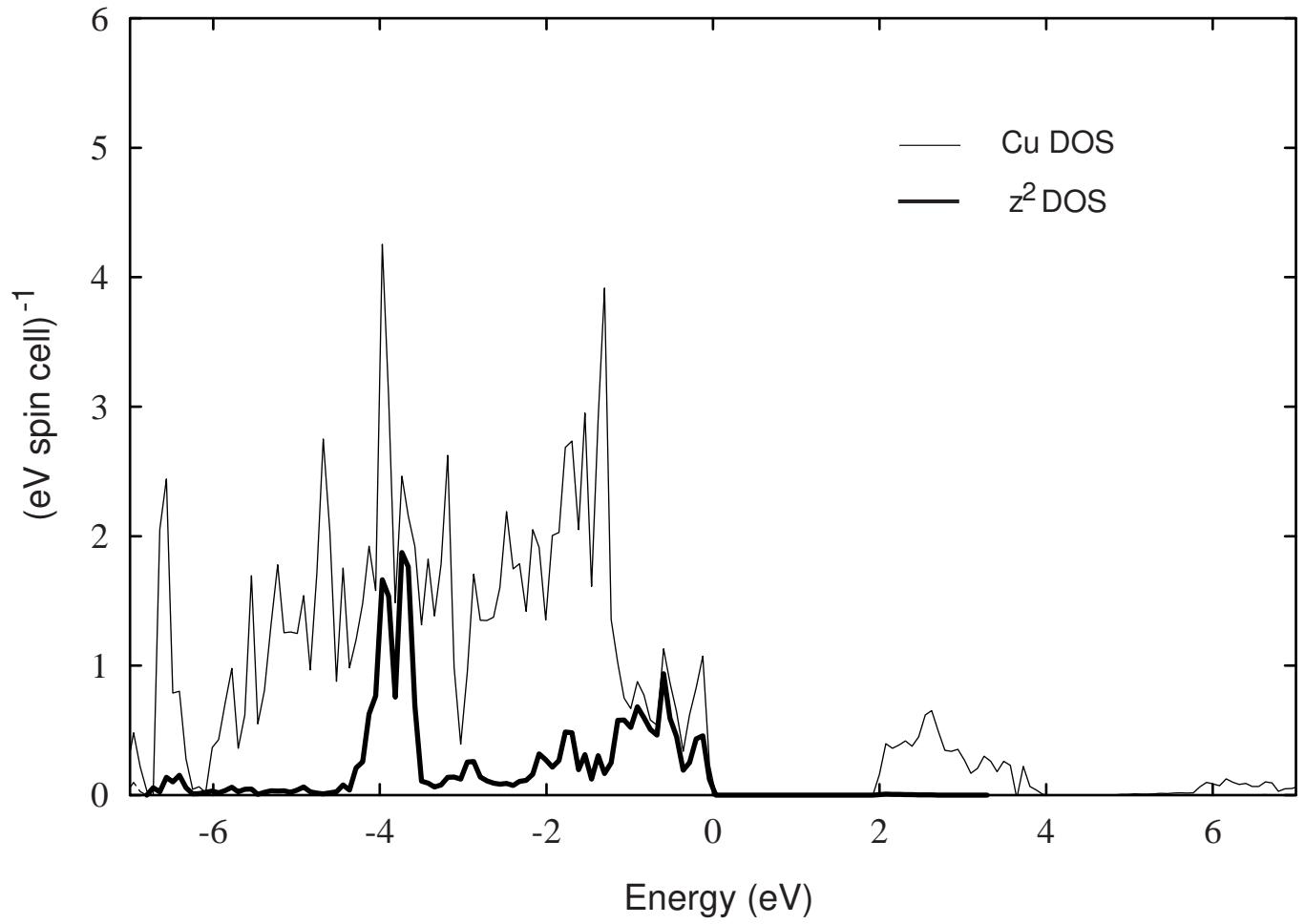


Figure 4e

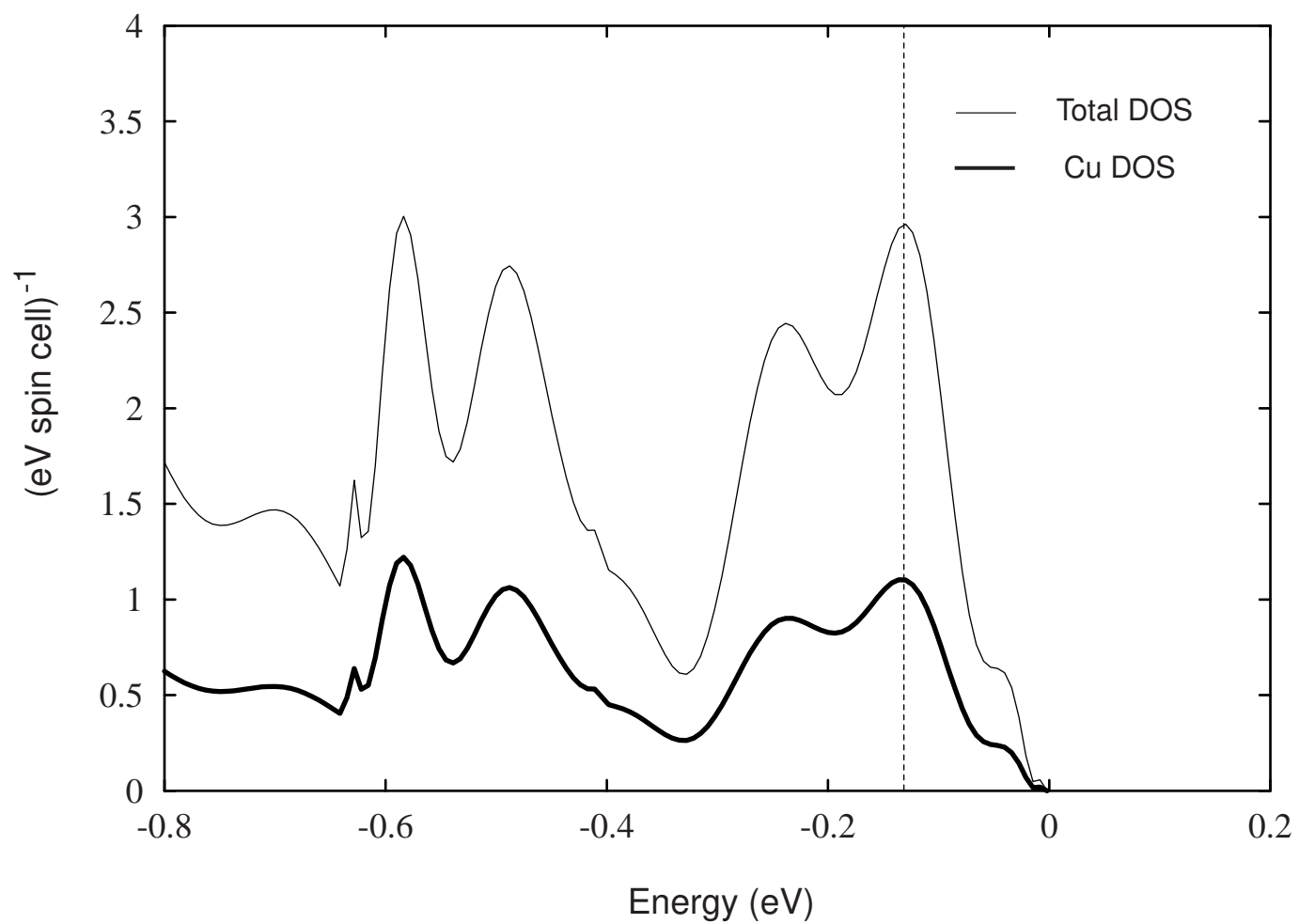


Figure 5a

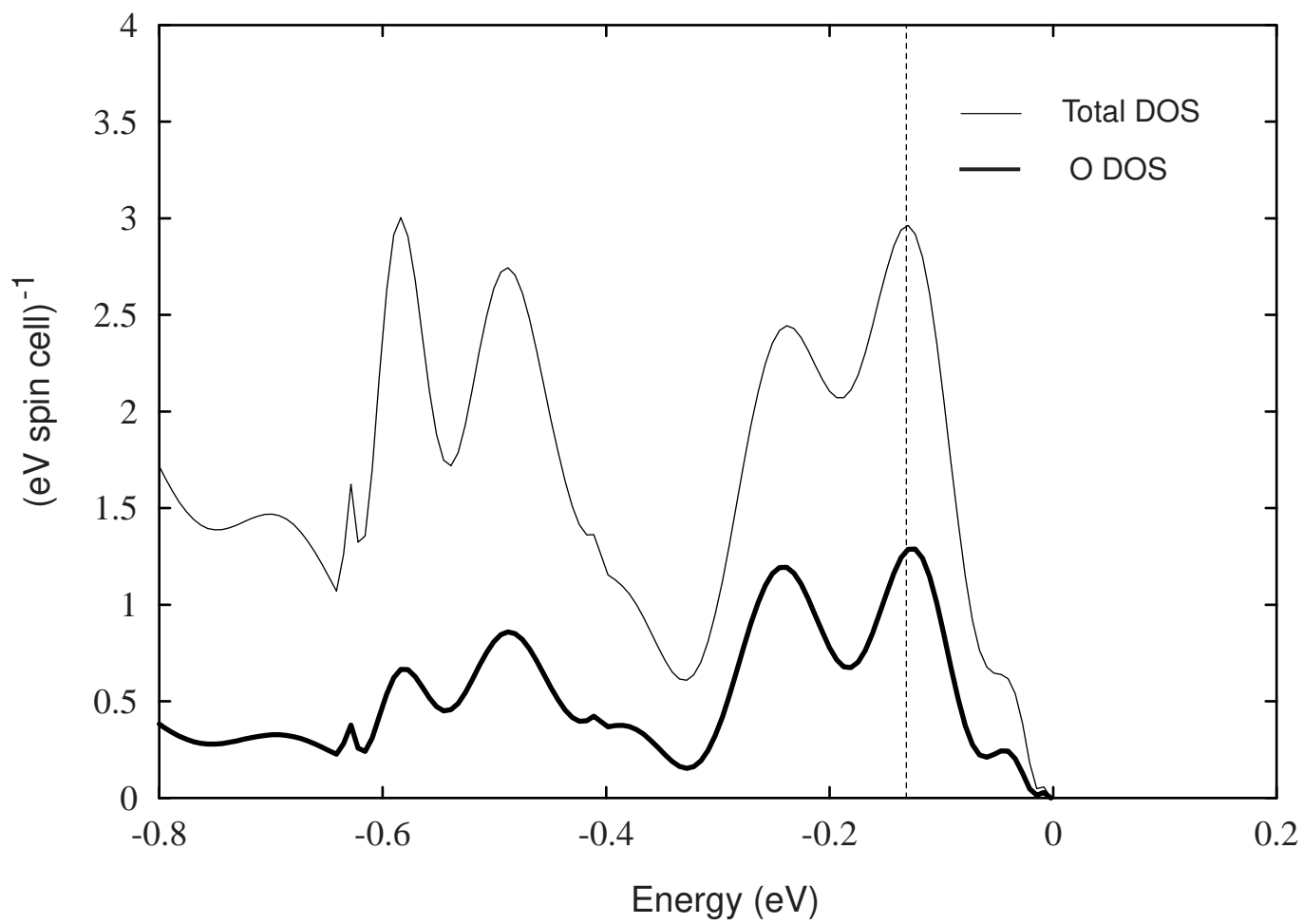


Figure 5b

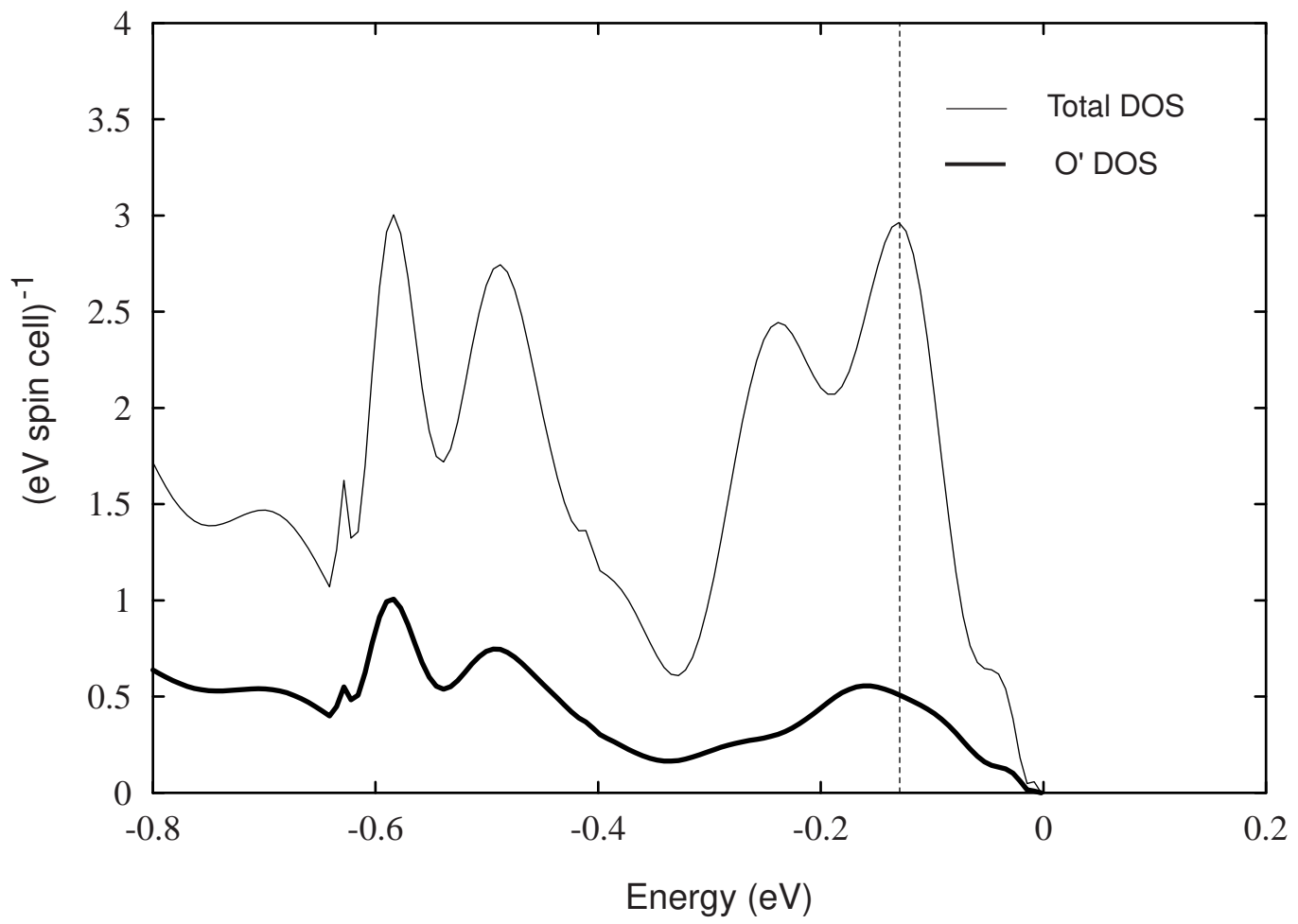


Figure 5c

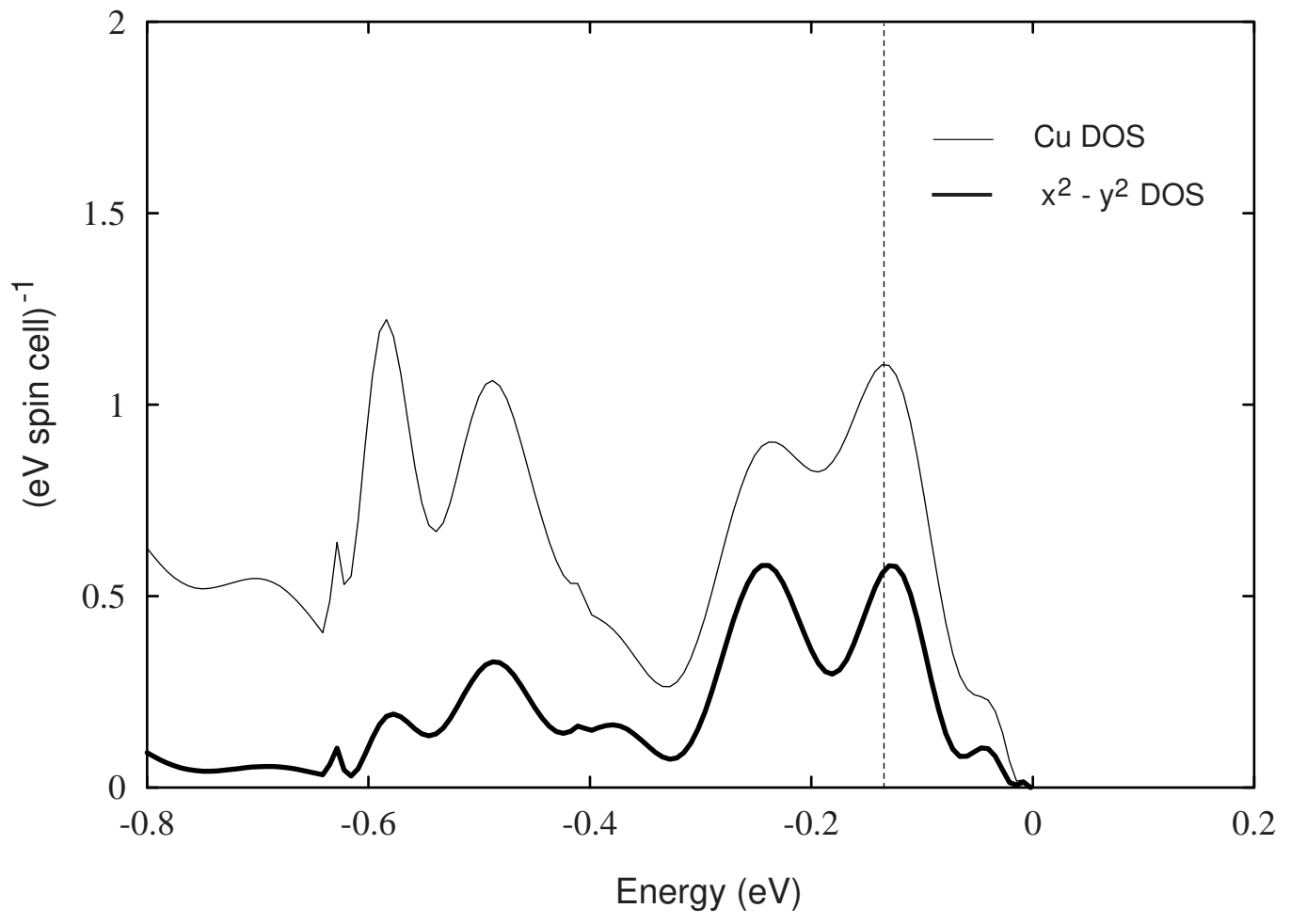


Figure 5d

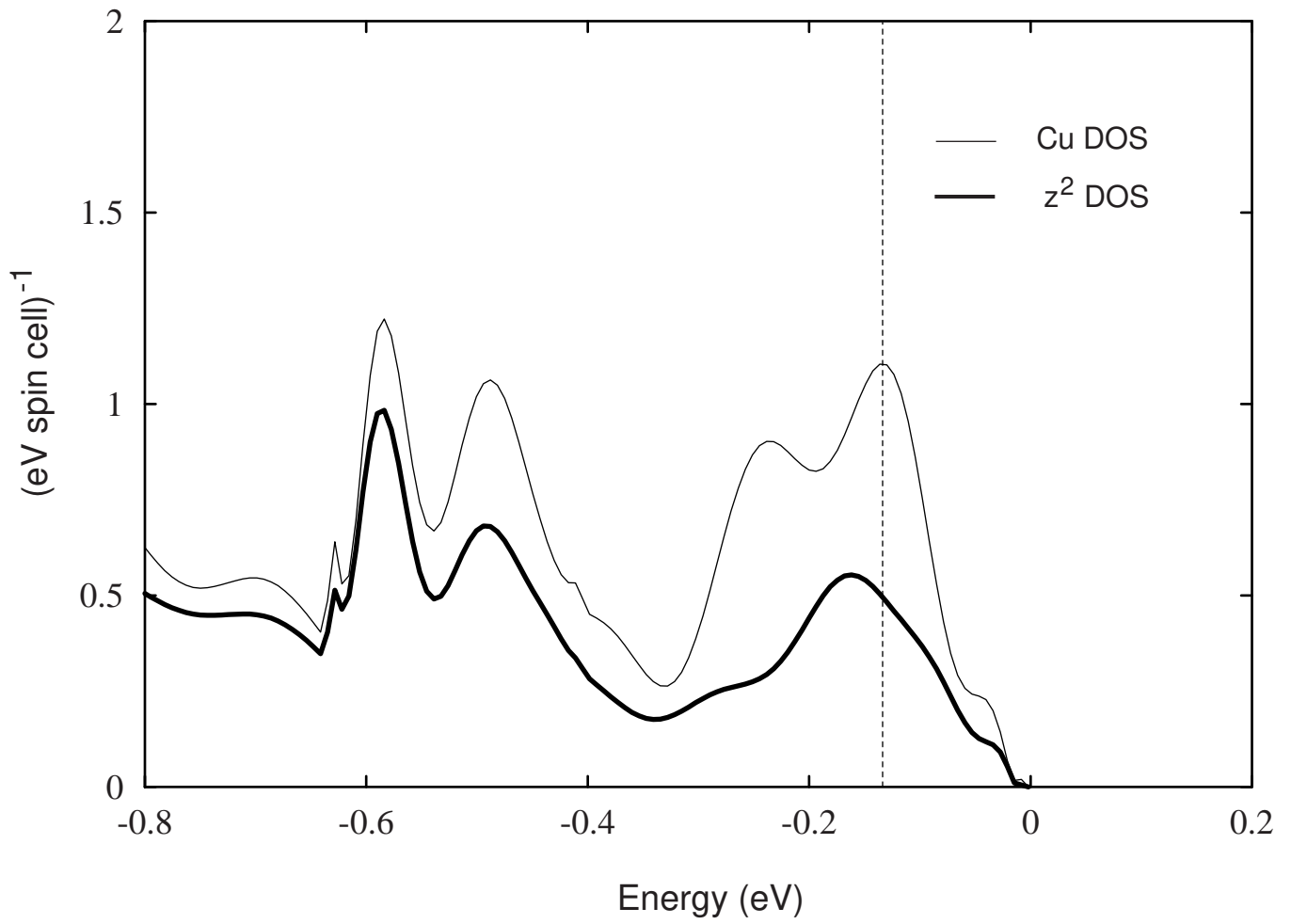


Figure 5e